J. Microbiol. Biotechnol. (2008), **18**(12), 1895–1902
doi: 10.4014/jmb.0800.210
First published online 29 July 2008

JOURNAL OF MICROBIOLOGY AND BIOTECHNOLOGY

Proteome Analysis for 3T3-L1 Adipocyte Differentiation

Atiar Rahman, Md, Suresh G. Kumar, Sung Hak Lee, Hee Sun Hwang, Hyun Ah Kim, and Jong Won Yun*

Department of Biotechnology, Daegu University, Kyungsan, Kyungbuk 712-714, Korea

Received: March 17, 2008 / Accepted: May 14, 2008

Adipose tissue is an important endocrine organ involved in the control of whole body energy homeostasis and insulin sensitivity. Considering the increased incidence of obesity and obesity-related disorders, including diabetes, it is important to understand thoroughly the process of adipocyte differentiation and its control. Therefore, we performed a differential proteome mapping strategy using two-dimensional gel electrophoresis combined with peptide mass fingerprinting to identify intracellular proteins that are differentially expressed during adipose conversion of 3T3-L1 pre-adipocytes in response to an adipogenic cocktail. In the current study, we identified 46 differentially expressed proteins, 6 of which have not been addressed previously in 3T3-L1 cell differentiation. Notably, we found that phosphoribosyl pyrophosphate synthetase (PRPS), a regulator of cell proliferation, was preferentially expressed in pre-adipocytes than in fully differentiated adipocytes. In conclusion, our results provide valuable information for further understanding of the adipogenic process.

Keywords: 3T3-L1, adipogenesis, differentiation, obesity, proteome, two-dimensional gel electrophoresis

Abbreviations used in this paper: (ARP1 actin B, ARP1 actin-related protein 1 homolog B; FABP, fatty acid binding protein; GPDH, glycerol-3-phosphate dehydrogenase; GST, glutathione S-transferase, mu 5; M6PRBP, mannose-6-phosphate receptor binding protein 1; MA, mature adipocytes; MPI, mannose phosphate isomerase; PA, pre-adipocyte; PRPS, phosphoribosyl pyrophosphate synthetase-associated protein 2.)

Adipose tissue, a key endocrine organ, is well recognized for its crucial role in the regulation of energy metabolism. Disorders of energy metabolism is one of the major causes of insulin resistance and its associated complications, such as hypertension, dyslipidemias, type 2 diabetes, cardiovascular diseases and obesity [2, 17]. Recently, there has been a dramatic increase in the incidence of obesity, now recognized as a major health concern, especially in the affluent world. Obesity is primarily a consequence of an increase in adipocyte size, due to increased cytoplasmic triglyceride deposition as well as elevated adipogenesis resulting in the formation of new adipocytes from precursor cells [9].

Because of the difficulty in studying adipogenesis *in vivo*, several *in vitro* models have been established to study the cellular and molecular events in adipogenesis [10]. Among these models, the 3T3-L1 pre-adipocyte cell line is the best characterized. This cell line provides a particularly useful *in vitro* model for studying the adipogenic program and understanding the molecular basis underlying the acquisition of insulin sensitivity [20]. When cultured in defined media, 3T3-L1 pre-adipocytes deposit triglyceride in cytoplasmic lipid droplets and express genes that are also expressed in adipocytes *in vivo*. We therefore chose pre-adipocytes and adipocytes of day 9 to examine the protein profile in greater detail. Genetically based approaches have led to the identification of key transcription factors in the complex transcriptional cascade that is activated during adipose conversion [25, 36]. These factors include peroxisome proliferator-activated receptor γ (PPAR γ), CCAAT/enhancer binding protein (C/EBP), and adipocyte differentiation and determination factor 1 (ADD1)-sterol regulatory element binding protein 1c (SREBP1c). Sequential activation of these transcription factors induces expression of adipocyte-specific genes, including enzymes, structural proteins, hormone receptors, and a variety of secreted factors involved in the regulation of energy homeostasis [30, 32].

Despite this promising progress, the detailed molecular events that occur during adipogenesis remain to be fully understood. Several studies with transcriptomics data from *in vitro* and *in vivo* experiments on obesity-related model systems have already provided insight into gene regulation during adipogenesis [4, 11, 19, 31]. This facilitates further detailed studies to dissect the molecular pathways involved in obesity.

Although the power of the DNA array is highly appreciated, the predictive value of mRNA expression is limited with respect to cellular physiology. Expression levels of mRNA often do not parallel the levels of protein expression from a particular gene [7, 12], and protein turnover and post-translational

*Corresponding author
Phone: 82-53-850-6556; Fax: 82-53-850-6559;
E-mail: jwyun@daegu.ac.kr

modifications, essential for cellular behavior, are not covered by the information obtained from DNA arrays [24]. Consequently, a broader understanding of the adipogenic process requires independent examination of protein expression and protein function complementing the mRNA expression analyses.

In the present study, we have used two-dimensional gel electrophoresis-based proteomic techniques to investigate changes and/or differential expression in the cellular proteins specifically involved in the conversion of 3T3-L1 pre-adipocytes into adipocytes. A limited number of reports have been documented for profiling of cellular proteins with a focus on 3T3-L1 differentiation [5, 29, 34, 35]. For example, Sidhu [29] identified a fall in actin content, whereas Welsh *et al.* [34] showed alterations in the expression of coactosin, a promoter of actin filament destabilization, and other signal molecules, including RhoGD-1, RhoGD-2, and EHD1. Involvement of α2 macroglobulin was also proposed by other investigators during the 3T3-L1 differentiation process by proteomic study [5]. However, those reports may not be enough to understand the adipogenic program in greater detail. Hence, we designed the current study to explore novel candidates and to obtain a more comprehensive view of fat cell differentiation.

Materials and Methods

Reagents and Cells

3T3-L1 mouse embryo fibroblasts were purchased from American Type Culture Collection (ATCC, Manassas, VA, U.S.A.). DMEM and FBS were purchased from Gibco BRL (Invitrogen, Carlsbad, CA, U.S.A.). Dexamethasone (DEX), 3-isobutyl-1-methylxanthine (IBMX), and insulin were purchased from Sigma Chemical (St. Louis, MO, U.S.A.).

Cell Culture and Differentiation of Adipocytes

3T3-L1 cells were maintained in several 100-mm Petri dishes with DMEM-containing 10% bovine calf serum until confluent. Two days after post-confluence (day 0), cells (pre-adipocytes) were harvested from half of the total number of dishes and the cells in the remaining dishes were stimulated to differentiate with 0.5 mM IBMX, 0.25 μM DEX, and 10 μg/ml insulin added to DMEM containing 10% FBS for 2 days (day 2). Cells were then switched to complete medium with 10 μg/ml insulin alone for another 2 days (day 4), followed by culturing with 10% FBS/DMEM until further analysis. Approximately 5 days after induction of differentiation, 90% of cells displayed the characteristic lipid-filled adipocyte phenotype. Cells in these conditions were harvested for further studies. All media contained 100 U/ml of penicillin and 100 μg/ml of streptomycin (Invitrogen). Cells were maintained at 37°C in a humidified 5% CO_2 atmosphere.

Oil Red O Staining

On day 8 of adipocyte differentiation induction, the formation of lipid droplets in cells was analyzed by Oil Red O staining as follows. After removal of culture medium, cells were washed twice with phosphate-buffered saline (PBS) and fixed with 10% formaldehyde at room temperature for 10 min. Then, the cells were incubated with a filtered Oil Red O (Sigma) solution (a mixture of three parts of 0.5% [w/v] Oil Red O in isopropanol and two parts of water) for 30 min at room temperature followed by washing with PBS twice, 70% ethanol once, and water twice. Cells were kept in water and photographed using an Olympus (Tokyo, Japan) microscope equipped with digital image acquisition (Figure not shown). Fat droplets in adipocytes were stained red.

Protein Extraction and Estimation

Extraction of proteins was done from the harvested cells. Because of the abundance of hydrophobic proteins and interference of lipid in the mature adipocytes, a modified rehydration buffer (8 M urea, 2 M thiourea, 4% CHAPS, 1 mM PMSF, 65 mM DTT, and 2% IPG buffer) was used to improve sample solubility, avoid protein precipitation, and achieve efficient extraction of total protein from cells. Total protein content was determined by the Bradford assay [3].

Two-Dimensional Gel Electrophoresis (2-DE)

2-DE images were made in triplicate for each adipocyte (a total of six gel images) and normalized prior to statistical analysis. The six gels of two groups were run at the same time and were performed in triplicate. IPG IEF of samples was carried out on pH 3–10 (NL), 17-cm IPG DryStrips in the PROTEIN IEF cell (Bio-Rad) using the protocol recommended by the manufacturer. IPG strips were rehydrated passively overnight in strip holders in 350 μl of rehydration solution containing 150 μg of protein sample. IEF was carried out as follows: 15 min at 250 V, 3 h at 250–10,000 V, 6 h at 10,000 V, and then held at 500 V until ready to run the second dimension. Briefly, 150 μg (30 μl) of the protein sample was mixed with 320 μl of rehydration solution containing 8 M urea, 2 M thiourea, 4% CHAPS, 1 mM PMSF, 65 mM DTT, and 2% IPG buffer. After focusing, the gel strips were equilibrated in a solution containing 6 M urea, 2% SDS, 1% DTT, 30% glycerol, and 50 mM Tris-HCl (pH 6.8) for 15 min, followed by further incubation in the same solution except for replacing DTT with 2.5% iodoacetamide for an additional 15 min. The equilibrated IPG strips were then gently rinsed with electrophoresis buffer. The gel strips were then placed on a 20×20 cm 12% polyacrylamide gel for resolution in the second dimension. The fractionation was performed with the Laemmli SDS-discontinuous system at a constant voltage of 20 mA per gel for 10 h, after which the separated gels were visualized by silver staining.

Image Capture and Analysis

Gels were imaged on a UMAX PowerLook 1120 (Maxium Technologies, Taipei, Taiwan), and the resulting 16-bit images were converted to TIF format prior to export and analysis. Intensity calibration was carried out using an intensity step wedge before gel image capture. Comparison of the images was performed using a modified version of ImageMaster 2D software V4.95 (Amersham Biosciences, Little Chalfont, Buckinghamshire, England). A standard gel was generated out of the images with the highest spot number. Spot quantities of all gels were normalized to remove nonexpression-related variations in spot intensity, so the raw quantity of each spot in a gel was divided by the total quantity of all of the spots in that gel that have been included in the standard. The results were evaluated in terms of spot OD. Statistical analysis of SPSS (ver. 11.0) by *t*-test allowed the study of proteins that were significantly increased or decreased after the conversion of the cell line. A $p<0.05$ was considered as significant. The relative OD and relative volume were also calculated to correct for differences in gel staining. Each spot intensity volume was processed by background

subtraction and total spot volume normalization; the resulting spot volume percentage was used for comparison.

Enzymatic Digestion of Proteins in Gels

Protein spots were enzymatically digested in-gel in a manner similar to that previously described by Shevchenko *et al.* [28] using modified porcine trypsin. Gel pieces were washed with 50% ACN to remove SDS, salts, and stain. The gel was then dried to remove solvent, rehydrated with trypsin (8–10 ng/μl), and incubated for 8–10 h at 37°C. The proteolytic reaction was terminated by adding 5 μl of 0.5% TFA. Tryptic peptides were recovered by combining the aqueous phase from several extractions of gel pieces with 50% ACN. After concentration, the peptide mixture was redissolved in the buffer and desalted using C_{18} ZipTips (Millipore, Watford, Herts, U.K.), and the peptides were eluted with 1–5 μl of ACN. An aliquot of this solution was mixed with an equal volume of a saturated solution of CHCA in 50% ACN, and 1 μl of the mixture was spotted onto a target plate.

Protein Identification

Protein analysis was performed using an Ettan MALDI-TOF (Amersham Biosciences). The peptides were evaporated with a N_2 laser at 337 nm using a delayed extraction mode. They were accelerated with a 20 kV injection pulse for TOF analysis. Each spectrum was the cumulative average of 300 laser shots. The search program ProFound, developed by The Rockefeller University (http://129.85.19.192/profound_bin/WebProFound.exe), was used for protein identification by peptide mass fingerprinting (PMF). Spectra were calibrated with trypsin autodigestion ion peak *m/z* (842.510 and 22,11.1046) as internal standards. Peptide masses were matched with the theoretical peptides of all proteins in the NCBI database using MASCOT search program (http://www.matrixscience.com). The following parameters were used for the database search: trypsin as cleaving enzyme; a maximum of one missed cleavage; iodoacetamide (Cys) as a complete modification; methionine as a partial modification; monoisotopic masses; and a mass tolerance of ±0.1 Da.

Western Blot Analysis

The differentially regulated levels of proteins of our interest were further confirmed by Western blot analysis as described below. An aliquot of the protein sample (30 mg) was diluted in 2× sample buffer (50 mM Tris [pH 6.8], 2% SDS, 10% glycerol, 0.1% bromophenol blue, and 5% β-mercaptoethanol) and heated for 5 min at 95°C before SDS-PAGE gel analysis (10–15%). Subsequently, they were transferred to a PVDF (Santa Cruz Biotechnology, Santa Cruz, CA, U.S.A.) membrane and incubated overnight with 5% blocking reagent (Amersham Biosciences) in TBS containing 0.1% Tween-20 at 4°C. The membrane was rinsed in four changes of TBS with Tween-20 (10 mM Tris-HCl, 150 mM NaCl, 0.1% Tween-20, pH 8.0), and incubated twice for 5 min and twice for 10 min in fresh washing buffer. It was then incubated for 2 h with blocking solution containing 1:200 dilution of primary antibody (goat anti-fatty acid binding protein [anti-FABP], rabbit anti-GST, anti-peroxiredoxin, and anti-SOD1; Santa Cruz Biotechnology). After four washes, the membrane was incubated again for 2 h in HRP-conjugated anti-goat IgG and anti-rabbit IgG/AP-conjugated secondary antibody (1:1,000; Santa Cruz Biotechnology) and developed using ECL (ECL Western blot analysis system kit; Amersham Biosciences)/BCIP/NBT (Sigma). The Western blot analysis was carried out by scanning with a UMAX PowerLook 1120 (Maxium Technologies, Akron, OH, U.S.A.) and digitalized using image analysis software (KODAK 1D; Eastman Kodak, Rochester, NY, U.S.A.).

Statistical Analysis

All experimental results were compared by one-way analysis of variance (ANOVA) using the Statistical Package of Social Science (SPSS, ver. 11.0) program, and the data were expressed as means±SE. Group means were considered to be significantly different at $p<0.05$, as determined by the technique of protective least-significant difference (LSD) when ANOVA indicated an overall significant treatment effect, $p<0.05$.

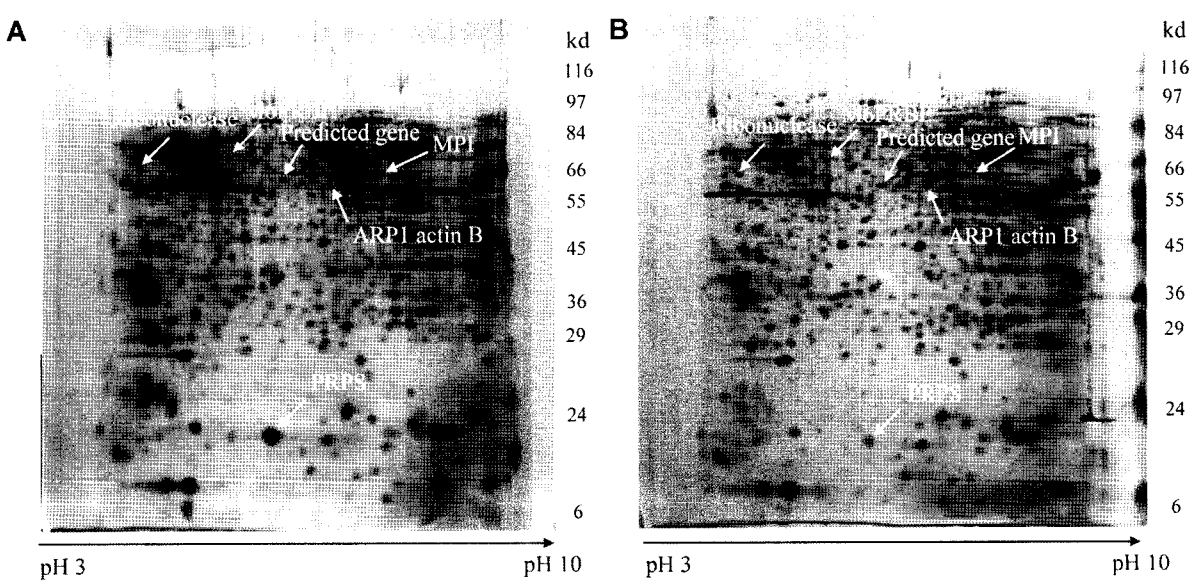

Fig. 1. 2D gel electrophoresis of total protein extracted from the cell: (**A**) pre-adipocyte and (**B**) mature adipocyte showing upregulated (ARP1 actin B, M6PRBP, ribonuclease, and predicted gene) and downregulated (MPI and PRPS) proteins.

Table 1. List of differentially expressed proteins (>1.5-fold) during conversion of 3T3-L1 pre-adipocytes into mature adipocytes.

Group ID	Protein[a]	Acc. No.[b]	Theoretical MW (kDa)	Theoretical pI	No. of matched peptides	Alterations (Vol%)		Fold change M/P	Coverage[c]	Z-score[d]
						Pre (P)	Mature (M)			
6010	GPDH	gi|387177	38.19	6.8	15	0.007±0.001	0.343±0.003	43.237	44	2.37
4182	GST	gi|6754086	27.02	6.9	11	0.079±0.010	0.165±0.013	2.097	41	2.33
2928	**ARP1 actin B**	gi|22122615	42.38	6.0	9	0.035±0.004	0.071±0.008	1.993	26	2.35
2535	**M6PRBP**	gi|13385312	47.36	5.5	10	0.082±0.007	0.153±0.037	1.873	27	2.39
2718	**Ribonuclease/ angiogenin inhibitor 1**	gi|31981748	51.51	4.7	8	0.093±0.025	0.167±0.010	1.791	24	2.42
5361	FABP	gi|6754450	15.46	6.1	6	0.200±0.015	0.336±0.024	1.676	41	1.40
2857	**Predicted gene, OTTMUSG00000010965**	gi|32822722	56.46	9.8	6	0.145±0.012	0.239±0.025	1.650	10	1.13
5147	Cu/Zn superoxide dismutase	gi|226471	15.91	6.0	6	0.344±0.060	0.482±0.018	1.503	44	1.76
2866	**MPI**	gi|14290579	47.18	5.5	5	0.085±0.012	0.054±0.006	0.635	12	1.27
5095	**PRPS**	gi|21450169	41.26	6.7	6	1.364±0.124	0.268±0.004	0.196	31	1.60

[a]For protein nomenclatures, see the Abbreviations section.
[b]Acc. No.: NCBInr database accession number.
[c]Coverage: percent of identified sequence to the complete sequence of the known protein.
[d]Z-score corresponds to the percentile of the search in the random match population: Z-score 1.65=95%, 2.33=99%, 3.09=99.9% confidence.

Results and Discussion

Adipocyte Differentiation

Pre-adipocytes were allowed to differentiate into mature adipocytes using adipogenic inducer with dexamethasone, IBMX and insulin. Intracellular fat contents during differentiation of 3T3-L1 cells were measured by Oil Red O staining. Microscopic examination of mature adipocytes showed 90% morphological changes from a fibroblastic to a spherical shape with accumulation of lipid droplets after the 8th day of differentiation (Figure not shown).

Protein Separation and Gel Spots Analysis

We have used silver stained 2-DE gels in conjunction with quantitative image analysis and PMF to investigate changes in protein expression during adipose conversion in 3T3-L1 cells. First, proteins were resolved in a broad-range IEF strip (pH 3–10, nonlinear gradient) in the first dimension followed by 12% SDS-PAGE gel in the second dimension. Fig. 1 shows a representative 2D pattern of 3T3-L1 pre-adipocytes and mature adipocytes (day 8 after differentiation). Positions of identified proteins on 2-DE gels were in the expected range of their theoretical p*I*s and molecular weights (MW; Table 1). These proteins were identified by MALDI-TOF and database searches with high confidence based on high scores and sequence coverage. Analysis of the gels showed about 1,600 individual spots ranging from 6 to 200 kDa masses between pH 3 and 10 (Fig. 1). A total of 46 proteins from the visualized spots were found to be differentially regulated, of which 40 spots were previously identified as adipogenic proteins by other investigators. The remaining 6 spots, to the best of our knowledge, were not examined in context of 3T3-L1 adipocyte differentiation (Table 1, indicated in bold). Fig. 2 shows four increased and two decreased spots with >1.5-fold expression during the course of the differentiation process and are classified as up- and down-regulated proteins. Among these, we found one spot that was abundantly expressed in pre-adipocytes, but was decreased dramatically following differentiation

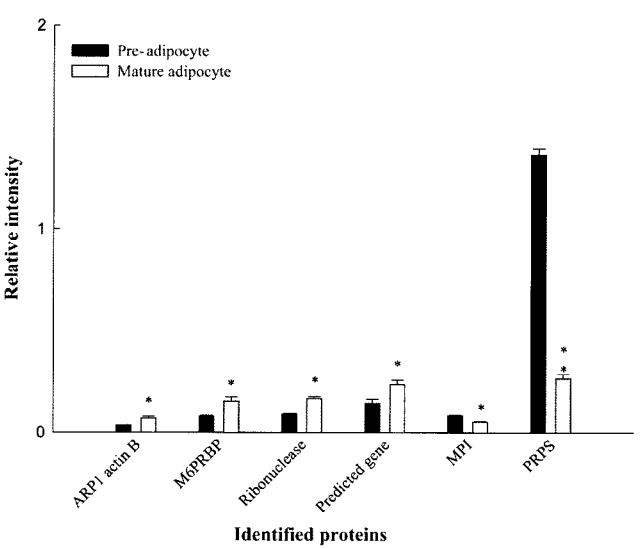

Fig. 2. Differential expression levels of proteins in pre- and mature adipocytes.
For protein nomenclatures, see the Abbreviations section. Values are mean ±SEM of three independent experiments, and are significant at $*p<0.05$, $**p<0.001$ when compared with pre-adipocytes.

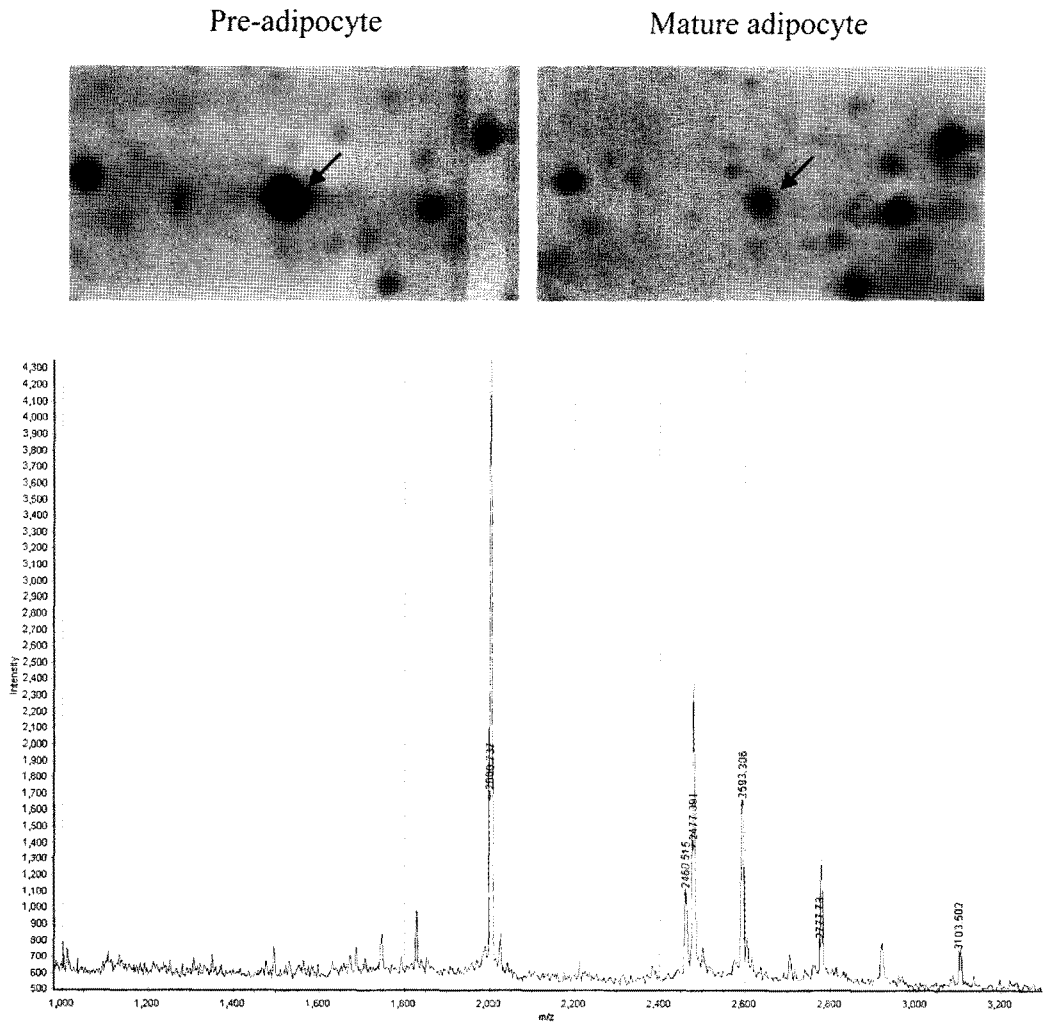

Fig. 3. MALDI-TOF spectra of phosphoribosyl pyrophosphate synthetase-associated protein 2 separated by 2D electrophoresis. Tryptic cleavage of the protein gave a mixture of peptides.

(Fig. 2). The MALDI-TOF analysis result identified this spot as phosphoribosyl pyrophosphate synthetase (PRPS)-associated protein 2, as shown in Fig. 3. Abundance of GPDH, a well-known marker protein for adipogenesis, in the gel was about 43-fold higher in the mature adipocytes [18, 37] when compared with 3T3-L1 pre-adipocytes, which indicates complete differentiation of pre-adipocytes into mature adipocytes.

Validation of 2-DE Results by Western Blotting

To validate the protein profile from our study, we carried out immunoblot analysis for four proteins (FABP, GST, peroxiredoxin, and SOD 1) as shown in Fig. 4. The well-correlated results of immunoblot and 2-DE profile validate and confirm the good agreement in the levels of protein. The protein profiling pattern was also compared with other studies [21, 22], which were found to be similar to our results.

Upregulated Proteins

Four proteins (namely, ARP1 actin-related protein 1 homolog B, Mannose-6-phosphate receptor binding protein 1, Ribonuclease/angiogenin inhibitor 1, and Predicted gene OTTMUSG00000010965) were newly identified, showing >1.5-fold upregulation after conversion of pre-adipocytes into mature adipocytes, which have not previously been explained in the context of 3T3-L1 cells. ARP1 actin-related protein 1 homolog B is a subunit of dynactin, a macromolecular complex consisting of 10 subunits whose molecular mass ranges from 22 to 150 kDa. It is involved in a diverse array of cellular functions, including ER-to-Golgi transport, the centripetal movement of lysosomes, spindle formation, and chromosome movement. Disregulation of this protein may lead to cell cycle misregulation [8]. Mannose-6-phosphate receptor binding protein 1 binds and interacts with the IGF-II/mannose-6-phosphate receptor, which are the constituents of the GLUT4 vesicle [16] in the adipocytes and helps in

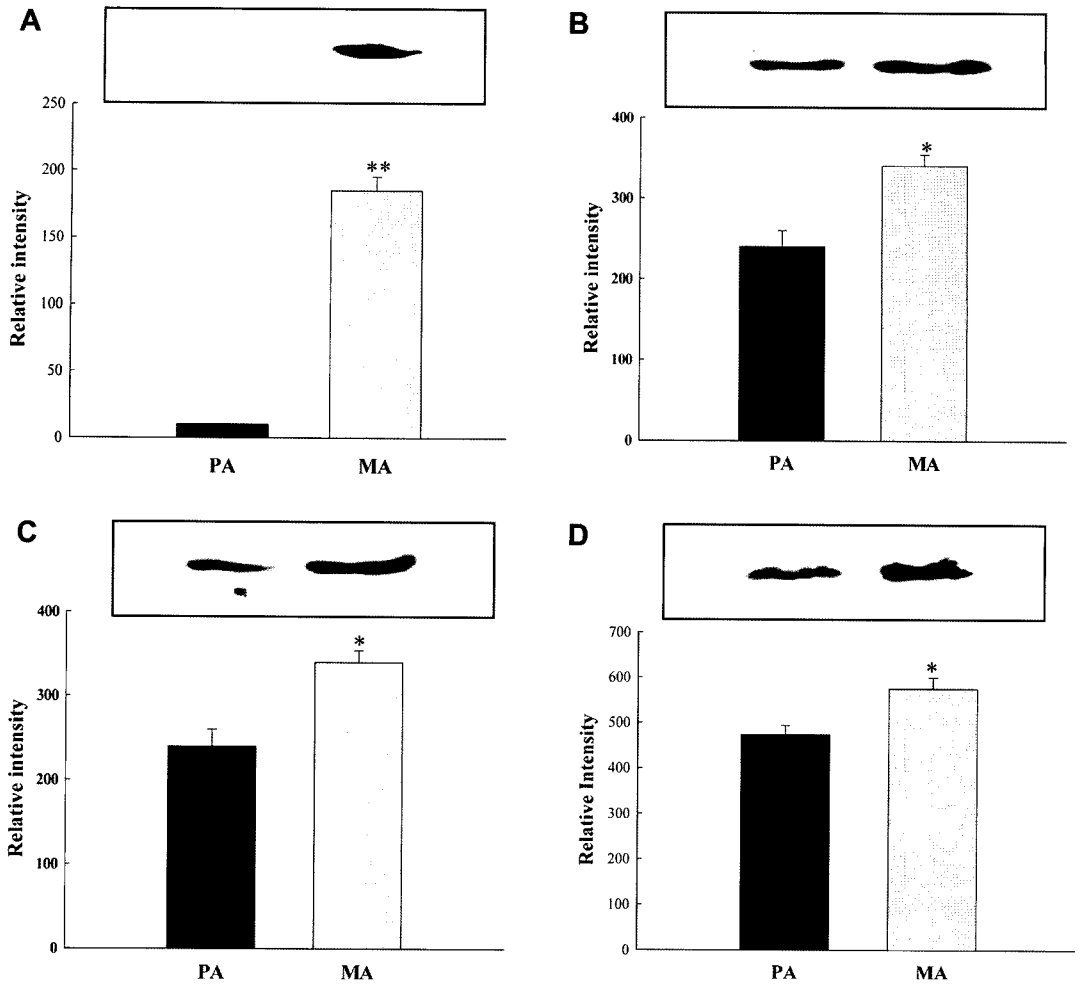

Fig. 4. Western blot analysis for protein levels of FABP (**A**), GST (**B**), Peroxiredoxin 1 (**C**), and SOD1 (**D**). Band density was digitized with software and mean ± SEM of three independent experiments, and are significant at $*p<0.05$, $**p<0.001$ when compared with pre-adipocytes.

translocation of GLUT4 to the surface of the membrane. Increased expression of this protein in the adipocytes may increase the number of GLUT4 on the surface in response to insulin, and hence triglyceride accumulation. Ribonuclease/angiogenin inhibitor 1 is presently used in molecular biology to stabilize preparations of polyribosomes and mRNA [26]. In the adipocytes, it may enhance the translation process for the development of adipocytes. It also inhibits ribonucleolytic and the angiogenic activities of angiogenin, which are interrelated [27]. The expression of predicted gene OTTMUSG00000010965 is not well characterized, and it may be involved in the adipocyte differentiation process. However, we have no evidence for this protein in connection with the adipogenic process.

Downregulated Proteins

Two proteins showed downregulation during differentiation; namely, mannose phosphate isomerase (MPI) and phosphoribosyl pyrophosphate synthetase-associated protein (PRPS) 2. MPI interconverts fructose-6-phosphate and mannose 6-phosphate, used for glycoconjugate biosynthesis. MPI mutations in humans impair protein glycosylation, causing congenital disorder of glycosylation Ib, but oral mannose supplements normalize glycosylation [6]. Expression of mannose phosphate isomerase was also observed during the 12-*O*-tetradecanoyl-phorbol-13-acetate (TPA)-induced differentiation of HL-60 cells into macrophage [14]. The involvement of this protein in 3T3-L1 differentiation is somehow obscure. It warrants further investigation to explore its function during differenitation. The expression of PRPS in pre-adipocytes is >5-fold ($p<0.001$) when compared to mature adipocytes, as shown in Fig. 3, and was identified by MALDI-TOF, which is quite significant in our results. Phosphoribosyl-pyrophosphate synthetase catalyzes the transfer of the terminal pyrophosphoryl group of ATP to ribose 5-phosphate to generate 5-phosphoribosyl 1(α)-pyrophosphate (PRPP). PRPP is required for the synthesis of purine and pyrimidine nucleotides. In nucleotide synthesis, PRPP is

used both for *de novo* synthesis and for the salvage pathway, by which bases are metabolized to nucleotides [33]. PRPS is thus a central enzyme in the metabolism of nitrogenous compounds and it is widely distributed in mammalian tissues [1, 13]. One report showed that the relatively low quantity of PRPP available in normal lymphocytes is a major factor limiting the synthesis of purine nucleotides and it is important for the maintenance of the quiescent state. Increased availability of PRPP may also be associated with proliferative activation of fibroblast-like cells [13]. Other studies have reported that the microarray analysis of gene expression in response to various stimuli showed PRPS involvement in DNA synthesis [15, 23]. Thus, 3T3-L1 undergoes growth arrest in the first induction itself, whereas the normal cells continue to proliferate, and hence it could be concluded that increased expression of PRPS-associated protein may be responsible for normal cell proliferation.

In conclusion, adipogenesis is a complex process that involves thousands of proteins at different stages of differentiation. Proteome analysis techniques allow the changes in steady-state levels of numerous proteins in a biological sample to be determined simultaneously. In our current study, 2-DE coupled with PMF was used to obtain novel candidates during 3T3-L1 differentiation. We identified six proteins in the context of adipogenesis (ARP1 actin B, Ribonuclease/angiogenin inhibitor 1, M6PRBP, predicted gene OTTMUSG00000010965, MPI, and PRPS), of which the expression of PRPS was more than 5-fold in pre-adipocytes than in mature adipocytes, indicating the probability of the involvement of PRPS in the cell proliferation of pre-adipocytes.

Acknowledgments

This work was supported by a grant from the Basic Research Program of the Korea Science and Engineering Foundation (R01-2008-000-10277-0). M. A. Rahman, S. G. Kumar, S. H. Lee, H. S. Hwang, and H. A. Kim were supported by a scholarship of the second stage of the Brain Korea 21 Project. The authors extend their thanks to Dr. Dong Soo Kim (Genomine Inc., Pohang, Korea) for his technical assistance in protein identification. Atar Rahman, Md and Suresh G. Kumar Contributed equally to this work.

References

1. Becker, M. A., P. Dicker, and E. Rozengurt. 1983. Mitogenic enhancement of purine base phosphoribosylation in Swiss mouse 3T3 cells. *Am. J. Physiol.* **244:** 288–296.
2. Biddinger, S. B. and C. R. Kahn. 2006. From mice to men: Insights into the insulin resistance syndromes. *Annu. Rev. Physiol.* **68:** 123–158.
3. Bradford, M. M. 1976. A rapid and sensitive method for the quantitation of microgram quantities of protein utilizing the principle of protein-dye binding. *Anal. Biochem.* **72:** 248–254.
4. Burton, G. R., Y. Guan, R. Nagarajan, and R. E. McGehee Jr. 2002. Microarray analysis of gene expression during early adipocyte differentiation. *Gene* **293:** 21–31.
5. Choi, K. L., Y. Wang, C. A. Tse, K. S. Lam, G. J. Cooper, and A. Xu. 2004. Proteomic analysis of adipocyte differentiation: Evidence that alpha2 macroglobulin is involved in the adipose conversion of 3T3 L1 preadipocytes. *Proteomics* **4:** 1840–1848.
6. DeRossi, C., L. Bode, E. A. Eklund, F. Zhang, J. A. Davis, V. Westphal, L. Wang, A. D. Borowsky, and H. H. Freeze. 2006. Ablation of mouse phosphomannose isomerase (Mpi) causes mannose 6-phosphate accumulation, toxicity, and embryonic lethality. *J. Biol. Chem.* **281:** 5916–5927.
7. Futcher, B., G. I. Latter, P. Monardo, C. S. McLaughlin, and J. I. Garrels. 1999. A sampling of the yeast proteome. *Mol. Cell. Biol.* **19:** 7357–7368.
8. Geigl, J. B., S. Langer, S. Barwisch, K. Pfleghaar, G. Lederer, and M. R. Speicher. 2004. Analysis of gene expression patterns and chromosomal changes associated with aging. *Cancer Res.* **64:** 8550–8557.
9. Gregoire, F. M. 2001. Adipocyte differentiation: From fibroblast to endocrine cell. *Exp. Biol. Med.* **226:** 997–1002.
10. Gregoire, F. M., C. M. Smas, and H. S. Sul. 1998. Understanding adipocyte differentiation. *Physiol. Rev.* **78:** 783–809.
11. Guo, X. and K. Liao. 2000. Analysis of gene expression profile during 3T3-L1 preadipocyte differentiation. *Gene* **251:** 45–53.
12. Gygi, S. P., Y. Rochon, B. R. Franza, and R. Aebersold. 1999. Correlation between protein and mRNA abundance in yeast. *Mol. Cell. Biol.* **19:** 1720–1730.
13. Hovi, T., A. C. Allison, K. Raivio, and A. Vaheri. 1977. Purine metabolism and control of cell proliferation. *Ciba Found Symp.* **48:** 225–248.
14. Juan, H. F., J. Y. Lin, W. H. Chang, C. Y. Wu, T. L. Pan, M. J. Tseng, K. H. Khoo, and S. T. Chen. 2002. Biomic study of human myeloid leukemia cells differentiation to macrophages using DNA array, proteomic, and bioinformatic analytical methods. *Electrophoresis* **23:** 2490–2504.
15. Kaida, A., Y. Ariumi, K. Baba, M. Matsubae, T. Takao, and K. Shimotohno. 2005. Identification of a novel p300-specific-associating protein, PRS1 (phosphoribosylpyrophosphate synthetase subunit 1). *Biochem. J.* **39:** 239–247.
16. Kandror, K. V. and P. F. Pilch. 1996. The insulin-like growth factor II/mannose 6-phosphate receptor utilizes the same membrane compartments as GLUT4 for insulin-dependent trafficking to and from the rat adipocyte cell surface. *J. Biol. Chem.* **271:** 21703–21708.
17. Kopelman, P. G. 2000. Obesity as a medical problem. *Nature* **404:** 635–643.
18. Moon, H. S., C. S. Chung, H. G. Lee, T. G. Kim, Y. J. Choi, and C. S. Cho. 2007. Inhibitory effect of (−)-epigallocatechin-3-gallate on lipid accumulation of 3T3-L1 cells. *Obesity* **15:** 2571–2582.
19. Nadler, S. T., J. P. Stoehr, K. L. Schueler, G. Tanimoto, B. S. Yandell, and A. D. Attie. 2000. The expression of adipogenic genes is decreased in obesity and diabetes mellitus. *Proc. Natl. Acad. Sci. USA* **97:** 11371–11376.

20. Ntambi, J. M. and Y. C. Kim. 2000. Adipocyte differentiation and gene expression. *J. Nutr.* **130:** 3122–3126.
21. Rahman, M. A., S. G. Kumar, S. W. Kim, H. J. Hwang, Y. M. Baek, S. H. Lee, H. S. Hwang, Y. H. Shon, K. S. Nam, and J. W. Yun. 2008. Proteomic analysis for inhibitory effect of chitosan oligosaccharides on 3T3-L1 adipocyte differentiation. *Proteomics* **8:** 569–581.
22. Renes, J., F. Bouwman, J. P. Noben, C. Evelo, J. E. Robben, and E. Mariman. 2005. Protein profiling of 3T3-L1 adipocyte differentiation and (tumor necrosis factor α-mediated) starvation. *Cell. Mol. Life Sci.* **62:** 492–503.
23. Rheem, D. M. 2002. Microarray-based expression profiling of normal and malignant immune cells. *Endocr. Rev.* **23:** 393–400.
24. Richards, J., F. Le Naour, S. Hanash, and L. Beretta. 2002. Integrated genomic and proteomic analysis of signaling pathways in dendritic cell differentiation and maturation. *Ann. NY Acad. Sci.* **975:** 91–100.
25. Rosen, E. D. and B. M. Spiegelman. 2000. Molecular regulation of adipogenesis. *Annu. Rev. Cell Dev. Biol.* **16:** 145–171.
26. Schneider, R., E. Schneider-Scherzer, M. Thurnher, B. Auer, and M. Schweiger. 1988. The primary structure of human ribonuclease/angiogenin inhibitor (RAI) discloses a novel highly diversified protein superfamily with a common repetitive module. *EMBO J.* **7:** 4151–4156.
27. Shapiro, R. and B. L. Vallee. 1987. Human placental ribonuclease inhibitor abolishes both angiogenic and ribonucleolytic activities of angiogenin. *Proc. Natl. Acad. Sci. USA* **84:** 2238–2241.
28. Shevchenko, A., M. Wilm, O. Vorm, and M. Mann. 1996. Mass spectrometric sequencing of proteins from silver stained gels. *Anal. Chem.* **68:** 850–858.
29. Sidhu, R. S. 1979. Two-dimensional electrophoretic analyses of proteins synthesized during differentiation of 3T3-L1 preadipocytes. *J. Biol. Chem.* **254:** 11111–11118.
30. Sorisky, A. 1999. From preadipocyte to adipocyte: Differentiation-directed signals of insulin from the cell surface to the nucleus. *Crit. Rev. Clin. Lab Sci.* **36:** 1–3.
31. Soukas, A., N. D. Socci, B. D. Saatkamp, S. Novelli, and J. M. Friedman. 2001. Distinct transcriptional profiles of adipogenesis *in vivo* and *in vitro*. *J. Biol. Chem.* **276:** 34167–34174.
32. Takahashi, M. 2001. Adipocytes as endocrine organ-adipocytokines and lipid metabolism. *J. Clin. Med.* **59:** 504–508.
33. Tatibana, M., K. Kita, M. Taira, S. Ishijima, T. Sonoda, T. Ishizuka, T. Iizasa, and I. Ahmad. 1995. Mammalian phosphoribosyl-pyrophosphate synthetase. *Adv. Enzyme Regul.* **35:** 229–249.
34. Welsh, G. I., M. R. Griffiths, K. J. Webster, M. J. Page, and J. M. Tavare. 2004. Proteome analysis of adipogenesis. *Proteomics* **4:** 1042–1051.
35. Wilson-Fritch, L., A. Burkart, G. Bell, K. Mendelson, J. Leszyk, S. Nicoloro, M. Czech, and S. Corvera. 2003. Mitochondrial biogenesis and remodeling during adipogenesis and in response to the insulin sensitizer rosiglitazone. *Mol. Cell. Biol.* **23:** 1085–1094.
36. Wu, Z., P. Puigserver, and B. M. Spiegelman. 1999. Transcriptional activation of adipogenesis. *Curr. Opin. Cell Biol.* **11:** 689–694.
37. Yang, Y., W. Shang, L. Zhou, B. Jiang, H. Jin, and M. Chen. 2007. Emodin with PPARgamma ligand-binding activity promotes adipocyte differentiation and increases glucose uptake in 3T3-L1 cells. *Biochem. Biophys. Res. Commun.* **353:** 225–230.